Subwavelength grating bimodal waveguide for refractive index sensing

Luis Torrijos-Morán and Jaime García-Rupérez
Nanophotonics Technology Center, Universitat Politècnica de València, Camino de Vera s/n, 46022 Valencia, Spain
jaigarru@ntc.upv.es

Abstract: Periodic subwavelength structures supporting two TE modes are presented as high performance sensors with bulk and surface sensitivities of 1375.5nm/RIU and 6.138nm/nm, respectively. A complete theoretical study is provided by numerical expressions and FDTD simulations.
OCIS codes: 130.0130, 280.0280.

1. Introduction and principle of operation

Subwavelength grating (SWG) periodic structures have been extensively studied in the literature during the last years for a huge range of applications and purposes. They offer several advantages in terms of refractive index (RI) engineering and sensing as a consequence of a stronger mode interaction with the surroundings than conventional waveguides [1,2]. Due to this fact, new sensor configurations including SWG elements in classic photonic sensing structures have emerged and opened new opportunities within this field, as in the case of SWG ring resonators [3], exhibiting significantly higher sensitivities than the original configurations. At the same time, bimodal interferometric waveguides have positioned as one of the best alternatives for biosensing due to their outstanding surface sensitivity in the detection of small target analytes [4,5].

In this work, we present a new sensor concept encompassing the benefits of SWG structures and modal interferometry [6]. The design is depicted in Fig. 1(a) where asymmetric input and output single-mode waveguides in the 'z' axis are needed in order to excite the even and odd TE parity modes in the bimodal region. The design parameters are Λ=290nm, DC=50% or 60%, w=1400nm and h=220nm in silicon over a silica substrate. Numerical simulations using MIT Photonics Band (MPB) software have been carried out. Calculated band diagrams present high dispersion properties for both modes at the end of the Brillouin zone. For low wavelengths at the beginning of the bimodal section, the even mode is more dispersive than the odd one, and thus the phase shift between both modes decreases as a function of wavelength. Conversely, as we increase in wavelength the even mode becomes non-dispersive and the phase shift trend changes. This effect determines the evolution of the phase shift as a function of wavelength, which has been numerically calculated. Larger wavelength shifts for changes in the cladding RI are obtained for those operating wavelengths where the phase shift slope is low. In addition, the phase shift is displaced towards lower wavelengths when the refractive index of the surroundings is increased, unlike what occurs at the beginning of the bimodal section.

2. Sensitivity analysis

In similar interferometric sensors, the sensitivity is usually expressed as the total phase shift produced for a given change in the cladding RI. However, this gives rise to long bimodal sections since the phase sensitivity scales with the length, producing large footprints which are not desired for integration purposes. Our approach is to measure the shift of the spectral dips produced at the output by the destructive interferences between both modes when the phase shift is a multiple of 2π radians. By correctly designing those spectral features at the critical sensitivity region, we can achieve high sensitive modal sensors of only few tens of microns long, in contrast to other bimodal sensors of even various millimeters. In this type of sensors such as ring resonators, the spectral bulk sensitivity is defined by Eq. (1), expressed in terms of phase shift multiplying and dividing by $\delta\varphi$:

$$S_b = \frac{\delta\varphi / \delta n_c}{\delta\varphi / \delta\lambda_f}. \tag{1}$$

The wavelength shift of the spectral dip is expressed by $\delta\lambda_f$ when a change in the cladding RI δn_c is produced. From this equation, we can observe how the sensitivity is inversely proportional to the phase shift derivative with respect to wavelength. Because of that, the sensitivity can reach high values as long as the phase shift slope gets closer to zero.

The surface sensitivity has been also evaluated as the relation between the spectral shift of the dip and the thickness of a certain layer with different refractive index than the cladding. Specifically a layer RI of n=1.48 under

an aqueous RI environment of n=1.36 has been considered. The sensor will present high surface sensitivities since the adding layer will fill the gaps between the SWG elements, maximizing the interaction with the propagating modes.

3. Results and conclusions

FDTD simulations have been performed in order to demonstrate the sensing performance of the SWG bimodal waveguide sensor. The design values are those detailed in the introduction, with two duty cycles to compare: 50% and 60%. Figure 1(b) shows the spectrum under different cladding RI scenarios and Fig. 1(c) depicts a comparison between the numerical sensitivity results using Eq. (1) and the sensitivity results obtained by FDTD simulations.

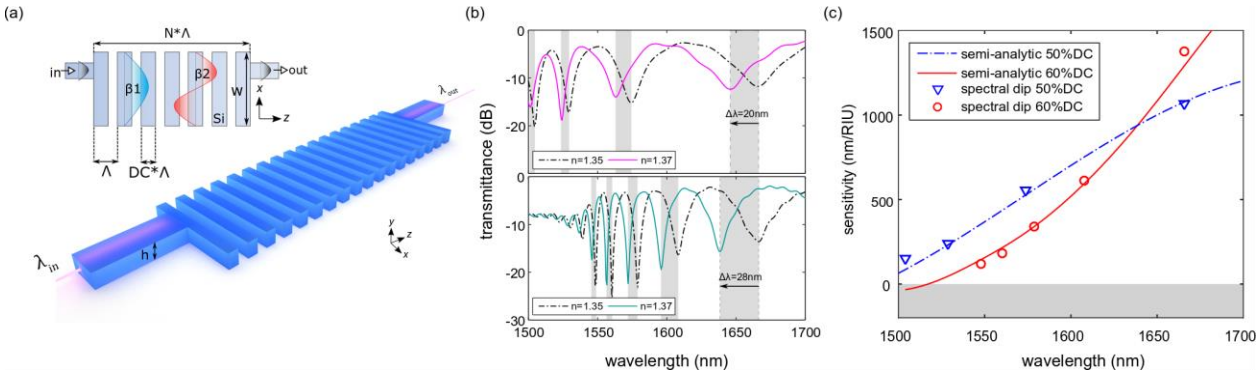

Fig. 1 (a) Schematic representation of the proposed SWG bimodal waveguide sensor. (b) Transmission spectra for 50% duty cycle (top) and 60% duty cycle (bottom) at different RI scenarios. (c) Comparison between the sensitivity results obtained in MPB using equation 1 (curves) and each spectral dip sensitivity calculated in FDTD (markers).

As it was explained previously, the sensitivity of each spectral dip clearly depends on wavelength, reaching maximum values of 1375.5 nm/RIU with a 60% duty cycle and for an operating wavelength around 1665nm. On the other hand, the duty cycle has a strongly influence in the sensitivity curves, since it determines the phase shift evolution as a function of wavelength. A lower value of 1070.1 nm/RIU has been obtained for 50% DC, representing a decrease of more than 20% in comparison to the results presented with 60% DC. Moreover, a good agreement between the numerical simulations in MPB using Eq. (1) and the tracking of the spectral dips by FDTD is obtained. These sensitivities improve by a factor above 2 those reported for SWG and multibox ring resonators [3,7] and by almost 6 the results obtained in convectional ring configurations. Regarding other interferometer sensors at the millimeters scale [8], lengths around 35μm and 64μm have been used in the simulations, what represents a step further in the integration of this type of interferometers in reduced devices. Furthermore, a surface sensitivity of 6.138nm/nm has been calculated for a 60nm-thick layer, which are, to the best of our knowledge, the highest reported in the literature for integrated photonic sensors on silicon. Experimental work is still being developed, although first evidences and results has been obtained recently supporting the theory explained in this paper.

4. References

1. J. Gonzalo Wangüemert-Pérez, P. Cheben, A. Ortega-Moñux, C. Alonso-Ramos, D. Pérez-Galacho, R. Halir, I. Molina-Fernández, D.-X. Xu, and J. H. Schmid, "Evanescent field waveguide sensing with subwavelength grating structures in silicon-on-insulator," Opt. Lett. **39**(15), 4442–4445 (2014).
2. J. G. Wangüemert-Pérez, A. Hadij-ElHouati, A. Sánchez-Postigo, J. Leuermann, D. X. Xu, P. Cheben, A. Ortega-Moñux, R. Halir, and Í. Molina-Fernández, "Subwavelength structures for silicon photonics biosensing," Opt. Laser Technol. **109**, 437–448 (2019).
3. J. Flueckiger, S. Schmidt, V. Donzella, A. Sherwali, D. M. Ratner, L. Chrostowski, and K. C. Cheung, "Sub-wavelength grating for enhanced ring resonator biosensor," Opt. Express **24**(14), 15672–15686 (2016).
4. K. E. Zinoviev, A. B. González-Guerrero, C. Domínguez, and L. M. Lechuga, "Integrated bimodal waveguide interferometric biosensor for label-free analysis," J. Light. Technol. **29**(13), 1926–1930 (2011).
5. D. Duval, A. B. González-Guerrero, S. Dante, J. Osmond, R. Monge, L. J. Fernández, K. E. Zinoviev, C. Domínguez, and L. M. Lechuga, "Nanophotonic lab-on-a-chip platforms including novel bimodal interferometers, microfluidics and grating couplers," Lab Chip **12**(11), 1987–1994 (2012).
6. L. Torrijos-Morán and J. García-Rupérez, "Single-channel bimodal interferometric sensor using subwavelength structures," Opt. Express **27**(6), 8168–8179 (2019).
7. E. Luan, H. Yun, L. Laplatine, Y. Dattner, D. M. Ratner, K. C. Cheung, and L. Chrostowski, "Enhanced sensitivity of subwavelength multibox waveguide microring resonator label-free biosensors," IEEE J. Sel. Top. Quantum Electron. **25**(3), (2019).
8. Z. Gu, J. S. Kee, Q. Liu, M. K. Park, and K. W. Kim, "Single-channel Mach-Zehnder interferometric biochemical sensor based on two-lateral-mode spiral waveguide," Opt. Express **22**(23), 27910 (2014).